Physically Meaningful Grid Analytics on Voltage Measurements using Graph Spectra

Mohini Bariya
Department of Electrical Engineering
University of California, Berkeley
mohini@berkeley.edu

Keith Moffat
Department of Electrical Engineering
University of California, Berkeley
keithm@berkeley.edu

Alexandra von Meier
Department of Electrical Engineering
University of California, Berkeley
vonmeier@berkeley.edu

***Abstract*—Time synchronized measurements of voltage magnitudes or phasors are increasingly common in electrical networks. Voltage measurement statistics are informative of the underlying network structure or topology making them useful for grid monitoring. However, this connection is poorly understood and many proposed voltage analytics are purely heuristic. We use graph theory to establish sound theoretical connections between voltage measurements and the structure of the underlying network. Our results are important for many applications, from topology estimation to missing data recovery. Based on this new theory, we discuss existing analytics, transforming them from heuristic to theoretically justified approaches, and introduce new analytics. We clarify all assumptions made, to indicate when analytics may fail or perform poorly. Our work enables voltage measurement streams to be transformed into physically meaningful, intuitive, visualizable, actionable information through simple algorithms.**

***Index Terms*—Smart grid, analytics, distribution monitoring, data-driven, sensor measurements, PMUs, topology**

I. Introduction

Time synchronized voltage measurements are increasingly common in the electric grid. Phasor measurement units (PMUs) which report time synchronized voltage phasors have been widely deployed on transmission networks[1]. Recently, specialized PMUs have been developed for distribution system monitoring [2]. Time synchronization enables geographically dispersed measurements to be aligned to generate a snapshot of the system. Sensor deployments are motivated by a need for better system monitoring and situational awareness. Sensors promise, but don't always deliver, greater system visibility because turning numerous, high resolution measurement streams into compact, intuitive, visualizable system information is nontrivial. Network structure or topology (the connectivity of network nodes) is a compact, visualizable, and important piece of system information that captures planned network changes, unplanned network changes that may indicate cyberattacks of switches, faults and other anomalies. Time synchronized voltage measurements from network nodes are intimately linked to network topology, though the exact theoretical connections, are poorly established. Instead, many heuristic approaches are proposed for system monitoring with voltages. Heuristics are defined as practical methods lacking theoretical justification. The advantages of heuristics are simple implementations and easy application to even a few measurement streams. However, their lack of theoretical justification makes it difficult to link their outputs to system physics, to understand the assumptions they make and when they may fail, and therefore to trust them. The approximate rank of voltage measurements [6], [7], [8], the correlations between nodal voltages [17], [18], and the principal components of nodal voltage measurements [19], [20], [21], [22], [23], [6] are popular heuristics for system monitoring. The work on these heuristics highlights their usefulness in particular applications, but doesn't establish the physical principle behind them. Instead, they have been experientially found insightful. Theoretically well founded analytics also exist in the literature. [28] and [29] use power flow linearizations to infer topology from voltage measurements. In [26], Ohm's Law and a known network model justify monitoring a projection of voltage measurements for anomaly detection. These works differ from ours as they are aimed at solving specific applications rather than creating an overall understanding of the measurements. Many generate results that are difficult to visualize, reducing their suitability for real application. Furthermore, they produce categorical rather than continuous outputs. At utilities, analytics will be applied to noisy data, in conditions where steady state assumptions do not always hold and used by human grid operators interested in changes in the grid state. Categorical outputs do not present intuition for the magnitude of detected changes and must always produce an absolutely correct answer.

In this work, we establish physics-based theory connecting voltage measurements properties in general—including rank, correlations, and clusters—to network topology allowing us to theoretically justify existing heuristic approaches—clarifying what they reveal of the system's physics and the assumptions they make—and propose novel analytics. The analytics we propose are continuous in their outputs so a human users must distinguish between changes indicative of real system changes from those due just to noise. Therefore the proposed analytics can be successful even if the assumptions underlying them do not perfectly hold at all times. Beyond specific analytics, our results lay the groundwork for better understanding and using grid voltage measurements, and are fundamental to a range of applications, including topology identification, phase identification, anomaly detection, and missing data recovery. They enable an otherwise overwhelming amount of voltage data to be transformed into intuitive, visualizable system information with relatively simple algorithms. This work is

978-1-7281-3103-0/20/$31.00

similar in spirit to [11], which also seeks to explain how simple analytics reveal aspects of the underlying system, but does not take a graph theoretic approach as we do.

A. Notation

- $\mathbb{A} \in \mathbb{C}^{n\times m}$ is an n-by-m complex-valued matrix.
- $A \in \mathbb{R}^{n\times m}$ is an n-by-m real-valued matrix.
- A^* and A^T are the conjugate and transpose of A respectively. $A^H = (A^*)^T$
- A_{ij} is the (i,j) element, A_{-i} is the i^{th} column, and A_{i-} is the i^{th} row of matrix A.
- $\mathcal{G} = (\mathcal{N}, \mathcal{E})$ is a graph with node set $\mathcal{N}$ and edge set $\mathcal{E}$. $|\mathcal{N}| = n$ and $|\mathcal{E}| = e$ is the number of nodes and edges respectively.

B. Measurement Model

Consider an electrical network represented by a graph $\mathcal{G}$ with n nodes. Let $\mathbb{V} \in \mathbb{C}^{n\times t}$ and $\mathbb{I} \in \mathbb{C}^{n\times t}$ denote nodal voltage and current injection phasors over t time points. We assume only $\mathbb{V}$ is measured. By Ohm's Law:

$$\mathbb{I} = \mathbb{Y}\mathbb{V} \leftrightarrow \mathbb{V} = \mathbb{Z}\mathbb{I} \tag{1}$$

$\mathbb{Y}$ is termed the network admittance matrix or the Laplacian of $\mathcal{G}$. It captures the complete network structure, consisting of connections and impedances. $\mathbb{Y}$ is symmetric and can be diagonalized as $\mathbb{Y} = \mathbb{U}D_\lambda\mathbb{U}^T$. $\mathbb{U}$ contains the eigenvectors of $\mathbb{Y}$ as columns, while D_λ is a diagonal matrix of the eigenvalues of $\mathbb{Y}$, denoted (in increasing order) $\lambda_1 \leq ... \leq \lambda_N$. By definition, $\lambda_1 = 0$. $\mathbb{Z}$ is the psuedoinverse of $\mathbb{Y}$ defined as:

$$\mathbb{Z} \triangleq \mathbb{W}D_{1/\lambda}\mathbb{W}^T, \ \mathbb{W} \triangleq \mathbb{U}^* \tag{2}$$

where $D_{1/\lambda}$ is a diagonal matrix containing the eigenvalues of $\mathbb{Z}$, denoted $\gamma_1 \leq ... \leq \gamma_N$. The eigenvalue set of $\mathbb{Z}$ contains the zero eigenvalues and the reciprocals of the *non-zero* eigenvalues of $\mathbb{Y}$. Therefore, $\mathbb{Z}$ preserves the null space of $\mathbb{Y}$. The rich field of graph theory has established many properties of graph Laplacian matrices and their eigenvalues and eigenvectors, some of which we will use. See [4] for a summary. In this work we use complex-valued, phasor measurements, but our results can be extended to magnitude measurements through power flow linearizations.

C. Assumptions

To derive various properties of voltage measurements, we make assumptions from the following set:

- **(A1)** Current injections are uncorrelated and have equal variance across nodes. That is:

$$\bar{\mathbb{I}} \triangleq (\mathbb{I} - \frac{1}{T}\mathbb{I}\mathbf{1}\mathbf{1}^T) \implies \bar{\mathbb{I}}\bar{\mathbb{I}}^H = \sigma_{\mathbb{I}}^2 I_n \tag{3}$$

  where I_n is the identity matrix and $\sigma_{\mathbb{I}}^2$ is the current injection variance at every node. This is a reasonable assumption since currents are driven primarily by power injections which should be statistically independent across nodes over short time scales.

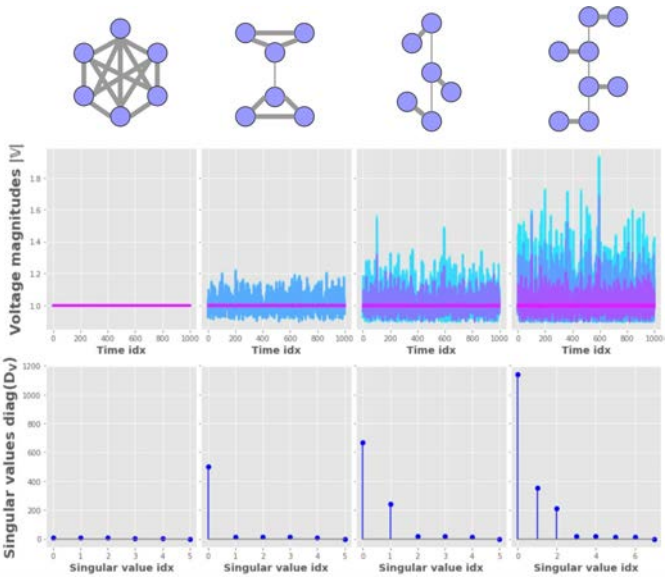

Fig. 1. Voltage measurements and singular values on test networks. Greater line thickness indicates lower admittance / higher impedance.

- **(A2)** $D_{1/\lambda}$ is approximately rank $k-1$ with $k-1$ equal eigenvalues and $n-k+1$ zero eigenvalues. That is:

$$\gamma_{N-k+1} \approx ... \approx \gamma_N \triangleq \gamma \tag{4}$$

$$0 = \gamma_1 \approx ... \approx \gamma_{N-k} \tag{5}$$

  The rationale for this assumption is based on graph theory and will be clarified in Section II.

Which results depend on which assumptions will be made clear in the text.

II. Voltage Data Rank

It is widely known that grid voltage measurements are approximately low rank: that is, $\mathbb{V}$ can be well approximated by a low rank matrix. This property motivates approaches to measurement compression, missing measurement recovery, and event detection [6], [7], [8]. It motivates a new approach to system identification and event localization in [10] and is used to detect cyberattacks in [9]. However, to the best of our knowledge, no prior work theoretically establishes the reason and extent of this observed phenomenon. We show the approximate rank of $\mathbb{V}$ can be connected to the structure of $\mathcal{G}$. Define $\bar{\mathbb{V}} \triangleq \mathbb{V} - \mathbb{Z}\bar{\mathbb{I}}$ to be the mean centered voltages with singular value decomposition $\mathbb{A}D_V\mathbb{B}^T$ where D_V is a digonal matrix containing the singular values of $\bar{\mathbb{V}}$. Then, under **(A1)**:

$$\bar{\mathbb{V}}\bar{\mathbb{V}}^H = \mathbb{A}D_V^2\mathbb{A}^H = \sigma_{\mathbb{I}}^2\mathbb{Z}\mathbb{Z}^H = \sigma_{\mathbb{I}}^2\mathbb{W}D_{1/\lambda}^2\mathbb{W}^T \tag{6}$$

The singular values of $\bar{\mathbb{V}}$ are the scaled eigenvalues of $\mathbb{Z}$, which are the reciprocals of the eigenvalues of $\mathbb{Y}$. The zero eigenvalues of Laplacian $\mathbb{Y}$ equals the number of connected components, or independent nodes clusters, in $\mathcal{G}$. Furthermore, a *near zero* eigenvalue of $\mathbb{Y}$ indicates a cluster or community of nodes that are highly connected to each other but "easily" separable (connected by low weight edges) from the rest of

$\mathcal{G}$ [12]. By (2), it is the near zero eigenvalues of $\mathbb{Y}$ that are the dominant eigenvalues of $\mathbb{Z}$. Therefore, if $\mathcal{G}$ contains k clusters or communities of nodes, $\bar{\mathbb{V}}$ will have $k-1$ dominant eigenvalues, meaning it can be well approximated by a rank k matrix.

This result is demonstrated in Fig. 1. The top row shows 4 networks with different topologies and realistic line impedances. Current injections are generated to statistically abide by **(A1)**. Voltage phasors are computed via (1). Notice the first network has a single community consisting of all the network nodes. Therefore $\bar{\mathbb{V}}$ has 0 dominant singular values. In other words, most of the variation in $\mathbb{V}$ is captured in the average voltage time series (indicated by the violet line in the first row of plots), and $\bar{\mathbb{V}}$ is near 0. This is evident in the tightness of the plot of $\mathbb{V}$ for this network. The other 3 networks have 2, 3, and 4 communities respectively. Inter-community lines are higher impedance than intra-community lines, indicated by line thickness in Fig. 1.

These results mean that the structure of $\mathcal{G}$ can inform various applications that rely on the rank of $\mathbb{V}$ such as the compressibility of $\mathbb{V}$ from $\mathcal{G}$, or the appropriate rank choice when recovering missing measurements in $\mathbb{V}$ through low rank matrix recovery. Conversely, the rank of $\mathbb{V}$ indicates the structure of the network and can alert us to changes in $\mathcal{G}$. Notice in Fig. 1 that the singular values of $\bar{\mathbb{V}}$ are more compact and easily visualized than $\mathbb{V}$. Now that we have given them physical meaning, they are an intuitive, visualizable quantity for system monitoring.

III. Voltage Clustering

Clustering voltage time series directly to monitor the structure of $\mathcal{G}$ is a known heuristic technique [13]. Yet, what it reveals about the structure of $\mathcal{G}$ in general, and why, has not been established. We theoretically justify this heuristic approach through the lens of spectral clustering: a popular technique for clustering the nodes of a graph. In brief, the results of spectral clustering say that given Laplacian $\mathbb{Y} = \mathbb{U}D_\lambda\mathbb{U}^T$ of $\mathcal{G}$, the nodes of $\mathcal{G}$ can be separated into k clusters that maximize inter-cluster edge weights and minimize intra-cluster edge weights by applying k-means to the *rows* of matrix $\mathbb{U}^{(k)} \in \mathbb{C}^{n\times k}$ where the columns of $\mathbb{U}^{(k)}$ are the first k eigenvectors of $\mathbb{Y}$ (the first k columns of $\mathbb{U}$)—that is the eigenvectors corresponding to $\lambda_{N-k}, ..., \lambda_N$. K-means clustering is a standard clustering algorithm which partitions data into a specified number of clusters, where each observation belongs to the cluster with the closest mean. Spectral clustering is derived through the relaxation of a non-convex optimization function over $\mathcal{G}$. See [14] for a more in-depth study. Here, we show that, under some assumptions, directly clustering the voltage time series $\bar{\mathbb{V}}_{1-}, ..., \bar{\mathbb{V}}_{n-}$ produces the same result as spectral clustering on $\mathbb{Y}$. Suppose $\mathcal{G}$ contains k node clusters. As discussed in Section II, it is then reasonable to assume **(A2)**, which means:

$$\bar{\mathbb{V}} \approx \gamma(\mathbb{U}^{(k)})^*(\mathbb{U}^{(k)})^H\bar{\mathbb{I}} \tag{7}$$

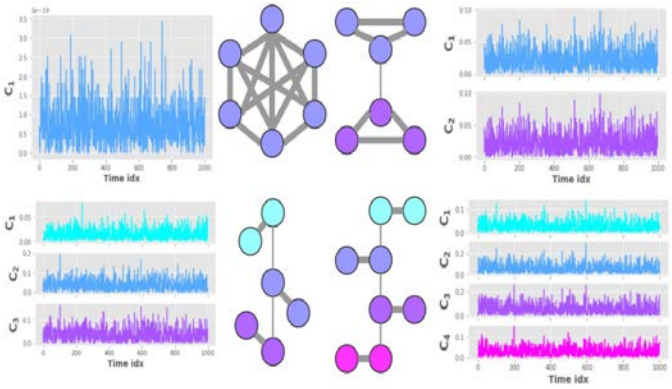

Fig. 2. Results of node clustering by clustering nodal voltage time series with k-means. Node color indicates cluster membership. Plots show centroids of mean centered voltages for each cluster.

The result of k-means clustering of $\mathbb{U}^{(k)}_{1-}, ..., \mathbb{U}^{(k)}_{n-}$ depends on the pairwise distances between rows [15]. A common distance metric is the Euclidean distance which is preserved when taking the conjugate and under multiplication by an orthogonal matrix. Under **(A1)**, we have:

$$||\mathbb{U}^{(k)}_{i-}(\mathbb{U}^{(k)})^H\bar{\mathbb{I}} - \mathbb{U}^{(k)}_{j-}(\mathbb{U}^{(k)})^H\bar{\mathbb{I}}||_2 = \sigma_{\mathbb{I}}||\mathbb{U}^{(k)}_{i-} - \mathbb{U}^{(k)}_{j-}||_2 \tag{8}$$

Together, (7) and (8) show that pairwise distances between rows are preserved between $\bar{\mathbb{V}}$ and $\mathbb{U}^{(k)}$, so applying k-means clustering to the rows of $\bar{\mathbb{V}}$ (the voltage time series $\bar{\mathbb{V}}_{1-}, ..., \bar{\mathbb{V}}_{n-}$) is equivalent to applying spectral clustering to $\mathcal{G}$. This result is demonstrated in Fig. 2, applied to the same test cases of Fig. 1. K-means clustering is applied to $\mathbb{V}$ and the resulting node cluster membership is indicated by node color. We see that the results of voltage clustering match those of spectral clustering. This result explains why voltage clustering techniques for coherency identification, such as [16], work at the transmission level, and extends the technique to distribution, even in the absence of inertial generators.

IV. Voltage Correlations

Using voltage correlations for system monitoring or topology estimation is a common heuristic technique [17], [18]. We propose an extension: clustering the rows of the voltage correlation matrix, denoted $\mathbb{S}^{(\mathbb{V})}$. We show that, under some assumptions, this is equivalent to spectral clustering on $\mathcal{G}$. Using assumption **(A1)**, and Eqs. (1)-(2), $\mathbb{S}^{(\mathbb{V})}$ is given by:

$$\mathbb{S}^{(\mathbb{V})} \triangleq \bar{\mathbb{V}}\bar{\mathbb{V}}^H = \sigma^2_{\mathbb{I}}\mathbb{U}^*D^2_{1/\lambda}\mathbb{U}^T \tag{9}$$

Incorporating **(A2)** gives:

$$\mathbb{S}^{(\mathbb{V})} \approx \sigma^2_{\mathbb{I}}\gamma^2(\mathbb{U}^{(k)})^*(\mathbb{U}^{(k)})^T \tag{10}$$

Since $(\mathbb{U}^{(k)})^T(\mathbb{U}^{(k)})^* = I_k$, by the results of Section III, clustering the rows of $\mathbb{S}^{(\mathbb{V})}$ will is equivalent to applying spectral clustering to $\mathcal{G}$. This result is visualized in Fig. 3, which shows the node cluster membership found by clustering the rows of $\mathbb{S}^{(\mathbb{V})}$, alongside $\mathbb{S}^{(\mathbb{V})}$ for each network. We see the clusters over $\mathbb{S}^{(\mathbb{V})}$ match the physical clusters in $\mathcal{G}$. At first, comparing the results of Sections III-IV seem to suggest clustering pairwise

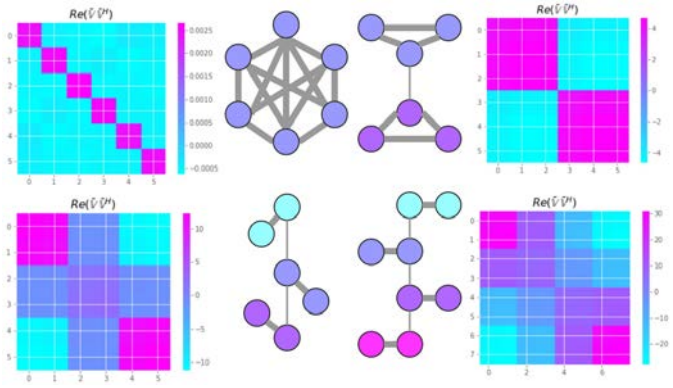

Fig. 3. Results of node clustering by clustering voltage correlation matrix $\mathbb{S}^{(\mathbb{V})} = \bar{\mathbb{V}}\bar{\mathbb{V}}^H$ with k-means. Node color indicates cluster membership. Plots show $Re(\mathbb{S}^{(\mathbb{V})})$ for each network.

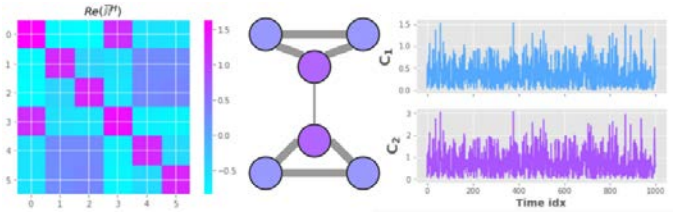

Fig. 4. Results of node clustering by clustering nodal voltage time series with k-means. Node color indicates cluster membership. Plots show centroids of mean centered voltages for each cluster. In this case, the current injections are correlated across nodes with the correlation matrix shown at left, leading to failure of the voltage clustering.

correlations from $\mathbb{S}^{(\mathbb{V})}$ is equivalent to clustering the voltage time series in $\bar{\mathbb{V}}$. However, notice that the assumption **(A2)** is applied to $D^2_{1/\lambda}$ to derive approximation (10), while it is directly applied to $D_{1/\lambda}$ to derive approximation (7). **(A2)** will tend to be more realistic on $D^2_{1/\lambda}$ than $D_{1/\lambda}$ because squaring will cause the largest k eigenvalues to dominate over the smaller, making (4) more accurate. Therefore, clustering over $\mathbb{S}^{(\mathbb{V})}$ will tend to be more robust than clustering over $\bar{\mathbb{V}}$.

V. Failure Cases

By understanding the assumptions underlying the heuristic analytic approaches, we can also understand when they will fail. This is important for a safety-critical infrastructure such as the electric grid, where operators will take rapid and impactful decisions based on the results of analytics. Fig. 4 shows how voltage time series clustering and voltage correlation clustering produce incorrect results when assumption **(A1)** does not hold. Current injections $\mathbb{I}$ are generated to have a particular correlation structure, visualized in Fig. 4. This is a pathological example, but current correlations can indeed stray far from **(A1)**. For example, the presence of distributed generation (such as PV) at multiple nodes can produce high correlations in current injections. Electric demand at different households has been observed to be correlated through a range of factors [30]. This will manifest in $\mathbb{I}$ injection correlations.

VI. Voltage PCA

Principal component analysis (PCA) transforms data to a new, lower dimensional subspace while maximizing the preserved variance. See [19] for more details. Applying PCA to voltage measurements is a widespread heuristic for grid monitoring. In [20], PCA is used to project many PMU voltage measurements onto a lower dimension subspace to reduce the data quantity and detect system changes. Linear systems theory is used to justify this approach, but no connection is made with the underlying graph structure. In [21], PCA is again used for event detection and localization, but without theoretical justification. In [24], PCA is applied to voltage angle measurements for fault detection. The advantages of PCA for reducing unwieldy data sets into tractable, informative and visualize-able ones has motivated its use in other grid measurement applications, such as bad data detection [22], [23]. However, to the best of our knowledge, the theory establishing the efficacy and physical meaning of PCA on voltage measurements is absent from the literature. Here, we connect PCA to spectral clustering. PCA allows us to reduce $\bar{\mathbb{V}} \in \mathbb{C}^{n\times t}$ to the lower dimensional $\hat{\mathbb{V}} \in \mathbb{C}^{n\times k}$. By definition, the principal components, denoted $\mathbb{P}$, are the conjugate eigenvectors of $\bar{\mathbb{V}}^H\bar{\mathbb{V}}$:

$$\bar{\mathbb{V}}^H\bar{\mathbb{V}} = \bar{\mathbb{I}}^H\mathbb{U}D^2_{1/\lambda}\mathbb{U}^H\bar{\mathbb{I}} \tag{11}$$

Assuming **(A1)**, $\bar{\mathbb{I}}^H\mathbb{U}$ has orthogonal columns. Therefore:

$$\mathbb{P} = \mathbb{U}^H\mathbb{I} \tag{12}$$

where the rows of $\mathbb{P}$ are the principal components. To find $\hat{\mathbb{V}}$, we project $\bar{\mathbb{V}}^H$ on the first k principal components. Assuming **(A2)**, this leads to:

$$\hat{\mathbb{V}} = \bar{\mathbb{V}}^*(\mathbb{P}^{(k)})^T = \sigma^2_{\mathbb{I}}\gamma\mathbb{U}^{(k)} \tag{13}$$

Therefore, the PCA transformed data is the scaled top k eigenvectors of $\mathbb{Y}$. Clearly from (13), clustering $\hat{\mathbb{V}}_{1-}, ..., \hat{\mathbb{V}}_{1-}$ is equivalent to clustering $\mathbb{U}^{(k)}_{1-}, ..., \mathbb{U}^{(k)}_{n-}$, which is spectral clustering. Therefore, PCA projects the measurements into a subspace with measurement clusters corresponding to node clusters in the graph $\mathcal{G}$.

This result is illustrated in Fig. 5. For every network, we choose $k = 2$. Notice that from a spectral clustering perspective, the choice of $k = 2$ means we are only bisecting $\mathcal{G}$. However, when plotting $\hat{\mathbb{V}} \in \mathbb{C}^{n\times 2}$, we see that the top two eigenvectors of $\mathbb{Y}$—contained in $\mathbb{U}^{(2)}$—are actually effective at separating the nodes into more defined, smaller clusters. In fact, in the plots we see that the nodes are well separated in terms of their true clusters in $\mathcal{G}$. In other words, $\mathbb{U}^{(2)}$ contains more information on $\mathcal{G}$ than a crude graph bisection.

VII. Conclusion

In this paper we establish fundamental properties of time synchronized voltage measurements from the electric grid using two simplifying assumptions. We use graph theory to show why phasor voltage measurements are low rank in most networks, and also provide intuition for the approximate

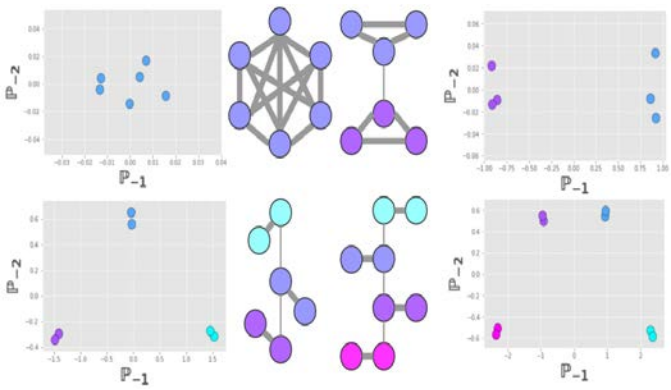

Fig. 5. PCA with $k = 2$ applied to nodal measurements in $\bar{\mathbb{V}}$. Notice how the projected data is well separated into the underlying node clusters in $\mathcal{G}$.

rank of the measurements in terms of the number of node clusters in the underlying network. This motivates analytics that use measurement rank to detect system changes, and also enables sounder application of low rank based compression and measurement recovery algorithms on voltage data. We also establish why clustering of raw voltage time series and voltage correlations reveals the underlying network structure. We show a similar result for PCA on voltage measurements. These results provide theoretical justification for existing heursitics and motivate the development of new analytics. Further, by giving physical meaning to simple, easily visualized computed quantities, such as clusters and principal components, we make them suitable for grid monitoring applications.

REFERENCES

[1] Overholt, P., Ortiz, D., & Silverstein, A. (2015). Synchrophasor technology and the DOE: Exciting opportunities lie ahead in development and deployment. IEEE Power and Energy Magazine, 13(5), 14-17.

[2] Von Meier, A., Culler, D., McEachern, A., & Arghandeh, R. (2014, February). Micro-synchrophasors for distribution systems. In ISGT 2014 (pp. 1-5). IEEE.

[3] J. P. Laglenne, B. Peifer, A. Regan, and L. Colangelo, Next-Gen Sensors for the Modern Grid, TD World, 08-Jul-2018.

[4] Chung, F. R., & Graham, F. C. (1997). Spectral graph theory (No. 92). American Mathematical Soc..

[5] Taylor, J. A. (2015). Convex optimization of power systems. Cambridge University Press.

[6] Wang, M., Chow, J. H., Gao, P., Jiang, X. T., Xia, Y., Ghiocel, S. G., ... & Razanousky, M. (2015, January). A low-rank matrix approach for the analysis of large amounts of power system synchrophasor data. In 2015 48th Hawaii International Conference on System Sciences (pp. 2637-2644). IEEE.

[7] Gao, P., Wang, R., Wang, M., & Chow, J. H. (2018). Low-rank matrix recovery from noisy, quantized, and erroneous measurements. IEEE Transactions on Signal Processing, 66(11), 2918-2932.

[8] Li, W., Wang, M., & Chow, J. H. (2017, July). Fast event identification through subspace characterization of PMU data in power systems. In 2017 IEEE Power Energy Society General Meeting (pp. 1-5). IEEE.

[9] Liu, L., Esmalifalak, M., & Han, Z. (2013, June). Detection of false data injection in power grid exploiting low rank and sparsity. In 2013 IEEE international conference on communications (ICC) (pp. 4461-4465). IEEE.

[10] Ardakanian, O., Yuan, Y., Dobbe, R., von Meier, A., Low, S., & Tomlin, C. (2017, July). Event detection and localization in distribution grids with phasor measurement units. In 2017 IEEE Power Energy Society General Meeting (pp. 1-5). IEEE.

[11] Escobar, M., Bienstock, D., & Chertkov, M. (2019, June). Learning from power system data stream. In 2019 IEEE Milan PowerTech (pp. 1-6). IEEE.

[12] McGraw, P. N., & Menzinger, M. (2008). Laplacian spectra as a diagnostic tool for network structure and dynamics. Physical Review E, 77(3), 031102.

[13] Mukherjee, A., Vallakati, R., Lachenaud, V., & Ranganathan, P. (2015, June). Using phasor data for visualization and data mining in smart-grid applications. In 2015 IEEE First International Conference on DC Microgrids (ICDCM) (pp. 13-18). IEEE.

[14] von Luxburg, Ulrike. A Tutorial on Spectral Clustering. https://arxiv.org/pdf/0711.0189.pdf

[15] Hartigan, J. A. (1975). Clustering algorithms.

[16] Adewole, A. C., & Tzoneva, R. (2015). Synchrophasor-based online coherency identification in voltage stability assessment. Advances in Electrical and Computer Engineering, 15(4), 33-43.

[17] Meier, R., Cotilla-Sanchez, E., McCamish, B., Chiu, D., Histand, M., Landford, J., & Bass, R. B. (2014, July). Power system data management and analysis using synchrophasor data. In 2014 IEEE Conference on Technologies for Sustainability (SusTech) (pp. 225-231). IEEE.

[18] Bariya, M., von Meier, A., Ostfeld, A., & Ratnam, E. (2018, April). Data-Driven Topology Estimation with Limited Sensors in Radial Distribution Feeders. In 2018 IEEE Green Technologies Conference (GreenTech) (pp. 183-188). IEEE.

[19] Shlens, J. (2014). A tutorial on principal component analysis. arXiv preprint arXiv:1404.1100.

[20] Xie, L., Chen, Y., & Kumar, P. R. (2014). Dimensionality reduction of synchrophasor data for early event detection: Linearized analysis. IEEE Transactions on Power Systems, 29(6), 2784-2794.

[21] Xu, T., & Overbye, T. (2015, November). Real-time event detection and feature extraction using PMU measurement data. In 2015 IEEE International Conference on Smart Grid Communications (SmartGridComm) (pp. 265-270). IEEE.

[22] Mahapatra, K., Chaudhuri, N. R., & Kavasseri, R. (2016, September). Bad data detection in PMU measurements using principal component analysis. In 2016 North American Power Symposium (NAPS) (pp. 1-6). IEEE.

[23] Mao, Z., Xu, T., & Overbye, T. J. (2017, September). Real-time detection of malicious PMU data. In 2017 19th International Conference on Intelligent System Application to Power Systems (ISAP) (pp. 1-6). IEEE.

[24] Wang, Z., Zhang, Y., & Zhang, J. (2011, July). Principal components fault location based on WAMS/PMU measure system. In 2011 IEEE Power and Energy Society General Meeting (pp. 1-5). IEEE.

[25] Smith, L. I. (2002). A tutorial on principal components analysis.

[26] Jamei, M., Scaglione, A., Roberts, C., Stewart, E., Peisert, S., McParland, C., & McEachern, A. (2017). Anomaly Detection Using Optimally Placed μPMU Sensors in Distribution Grids. IEEE Transactions on Power Systems, 33(4), 3611-3623.

[27] Jamei, M., Scaglione, A., & Peisert, S. (2018, October). Low-resolution fault localization using phasor measurement units with community detection. In 2018 IEEE International Conference on Communications, Control, and Computing Technologies for Smart Grids (SmartGridComm) (pp. 1-6). IEEE.

[28] Deka, D., Backhaus, S., & Chertkov, M. (2017). Structure learning in power distribution networks. IEEE Transactions on Control of Network Systems, 5(3), 1061-1074.

[29] Bolognani, S., Bof, N., Michelotti, D., Muraro, R., & Schenato, L. (2013, December). Identification of power distribution network topology via voltage correlation analysis. In 52nd IEEE Conference on Decision and Control (pp. 1659-1664). IEEE.

[30] Tascikaraoglu, A., Sanandaji, B. M. (2016). Short-term residential electric load forecasting: A compressive spatio-temporal approach. Energy and Buildings, 111, 380-392.